Volume 15, Issue 3, 152529 (1-9)

Iranian Journal of Catalysis (IJC)

https://doi.org/10.57647/j.ijc.2025.1503.29

Synthesis of MXene as a modifier of screen-printed carbon electrode for the measurement of clonazepam as an anesthetic drug

Mahbobe Eghbali[1], Esmail Sohouli[2], Amin Moradi-hsanabad[3], Gholamreza Mostafai[4], Mehdi Rahiminasarabadi[5], Reza Hosseiniara[6], Maryam Akbari[7], Ali Sobhani nasab[8,*], Amir Hossein Mohammadi[6,*]

[1]*School of Medicine, Kashan University of Medical Sciences, Kashan, Iran.*
[2]*2Department of Chemistry, Faculty of Science, Electrochemical Sensors Research Laboratory, Shahid Rajaee Teacher Training University, Lavizan, Tehran, Iran.*
[3]*Autoimmune diseases research center, Kashan University of Medical Sciences, Kashan, Iran.*
[4]*Department of Environmental Health, School of Health, Kashan University of Medical Sciences, Kashan, Iran.*
[5]*Institute of Electronic and Sensor Materials, TU Bergakademie, Freiberg, Germany.*
[6]*Research Center for Biochemistry and Nutrition in Metabolic Diseases, Institute for Basic Sciences, Kashan University of Medical Sciences, Kashan, Iran*
[7]*Department of Surgery, School of Medicine, Kashan University of Medical Sciences, Kashan, Iran.*
[8]*Physiology Research Center, Institute for Basic Sciences, Kashan University of Medical Sciences, Kashan, Iran.*

[*]**Corresponding authors:** ali.sobhaninasab@gmail.com, 921811353023s@gmail.com

Original Research

Received:
8 November 2024
Revised:
25 April 2025
Accepted:
1 June 2025
Published online:
1 July 2025
Published in issue:
30 September 2025

Abstract:

Benzodiazepines are psychoactive compounds with sedative, hypnotic, anti-anxiety, anticonvulsant, muscle relaxant, and anti-inflammatory effects. The increasing use of benzodiazepine anesthetics in recent years highlights the importance of analyzing these drugs in biological fluids to ensure therapeutic effectiveness, monitor concentrations, identify toxic levels, minimize negative effects, and enhance understanding of their function in biological matrices. In this study, we present the fabrication and electrochemical assessment of a novel sensing platform with high sensitivity to the drug clonazepam (CLZP). The synthesized electrode modifier, comprising MXE, was characterized using Fourier transform infrared spectrometry, scanning electron microscopy, and XRD techniques. The electrode modifier was applied to a screen-printed carbon electrode surface using the drop-casting method. The modification of the electrode with the proposed nanocomposite led to an increase in the current observed during the reduction of clonazepam and a decrease in the peak potential required for reduction. This enhancement in the electrochemical response to clonazepam reduction suggests a synergistic effect between MXE and the screen-printed carbon electrode. In optimal circumstances, the developed sensor displayed a direct relationship between the reduction peak current and CLZP concentrations within the 1 to 100 μM range, achieving a detection limit of 0.3 μM. The sensor was successfully employed for the accurate measurement of CLZP in human serum and pharmaceutical samples, demonstrating excellent sensitivity, enduring stability, and consistent reproducibility.

Keywords: Anesthetic drugs; Benzodiazepine; Clonazepam; Magzen; Printed carbon electrode

1. Introduction

Clonazepam, a benzodiazepine, is widely prescribed for managing anxiety disorders, panic attacks, seizures, and certain sleep-related issues. It is also used off-label to treat conditions like restless leg syndrome and REM sleep behavior disorder. Typically, treatment starts with a low dose that is gradually adjusted according to the patient's response and the specific disorder. For adults dealing with anxiety

or panic disorders, recommended daily dosages generally range from 0.25 to 2 mg, divided into two or three administrations. Common side effects include drowsiness, dizziness, impaired coordination, and fatigue, while less frequent but more serious effects may involve memory issues, confusion, depression, and changes in sexual desire. Abrupt discontinuation of clonazepam can trigger withdrawal symptoms such as anxiety, insomnia, and seizures, emphasizing the need for gradual tapering [1–4].

Various analytical methods have been employed to determine clonazepam in pharmaceutical formulations and biological samples. High-Performance Liquid Chromatography (HPLC) [5], Gas Chromatography (GC) [6], Liquid Chromatography-Mass Spectrometry (LC-MS) [7], and Spectrophotometry [8] are among the most common methods. Despite their popularity, each method has notable limitations affecting their routine use. HPLC, for instance, demands considerable time due to lengthy separation and detection steps, with complex sample preparation procedures adding to the overall workload and cost, given the expensive equipment and maintenance. GC is primarily suitable for volatile compounds or those that require derivatization, and clonazepam's heat sensitivity poses additional challenges in gas chromatography. Moreover, precise temperature control and careful column selection are necessary, complicating method development. LC-MS offers high sensitivity but is limited by the high cost of instruments, the complexity of operation, and matrix effects like ion suppression or enhancement that can impact result accuracy. Spectrophotometric methods, while simpler, struggle with specificity issues, as excipients and impurities in samples can interfere with measurements. They also tend to have lower sensitivity, requiring higher analyte concentrations to achieve dependable results [8–11].

Among various analytical methods, electrochemical determination of clonazepam offers several advantages, including high sensitivity, selectivity, simplicity, and cost-effectiveness [12–14]. In recent years, have gained significant attention for their wide-ranging applications in various fields, including Nanomedicine [15], Energy Storage and Conversion [16], Environmental Remediation [17], Catalysis [18], Electronics and Optoelectronics [19] and electrochemical sensors [20] due to their unique properties and potential for enhancing performance. Several types of nanomaterials have been extensively employed for the modification of electrochemical sensors and biosensors. Carbon-based nanomaterials [21], Metal nanoparticles [22], Metal oxide nanoparticles [23], Quantum dots [24], and Molecularly imprinted polymers (MIPs) [25] are some commonly utilized nanomaterials. In 2011, Prof. Gogotsi and colleagues introduced a novel category of 2D materials called MXEs (MXE). MXE phases or titanium aluminium carbide (Ti_3AlC_2) are high-melting non-oxide compounds with a hexagonal layered structure [26, 27]. These materials are distinguished by their remarkable electrical conductivity, hydrophilic surface characteristics, comparatively good environmental stability, tolerance to damage, nontoxic effect, low cost, and ease of synthesis [28]. MXEs are produced through the selective removal of "A" layers from layered carbides or carbonitrides, leading to the creation of 2D structures. The precursor compounds, referred to as MAX phases, have a general formula of Mn+1AXn (where n = 1, 2, 3). In this formulation, M represents a transition metal, A signifies a group IIIA and IVA element from the periodic table, and X can be either carbon (C)/or nitrogen (N) [29]. MXE has several unique characteristics that make it highly suitable for electrochemical sensors. Its excellent electrical conductivity enables fast electron transfer, and its simple synthesis process, good dispersibility, and stability facilitate easy electrode modification. MXE also serves as a durable, eco-friendly, and cost-effective material for printing complex structures, supporting the fabrication of multifunctional devices. Its high stretchability and biocompatibility make it ideal for flexible, wearable health-monitoring sensors. Additionally, MXE's 2D structure and rich surface chemistry allow easy integration with functional materials and biomolecules, enhancing its application in various electrochemical and biosensor technologies [30]. There are numerous applications of electrochemical sensors made from MXE materials, including the detection of biomarkers, drugs, and environmental pollutants [29].

In this study, Magzen was successfully synthesized and used to create a new sensor based on printed carbon electrodes. The sensor was designed to determine CLZP electrochemically using DPV. The study thoroughly investigated and optimized the experimental parameters influencing the sensor's voltammetric response. Under optimal conditions, the newly proposed sensor demonstrated heightened sensitivity and superior stability compared to CLZP. Additionally, it was successfully applied to detect CLZP in real samples. This technique offers several advantages, including simplified and rapid sensor fabrication, enhanced sensitivity, expanded detection linear range, and a low detection limit.

2. Experimental

2.1 Materials and equipment

Pharmaceutical grade CLZP with a purity exceeding 99.9% was acquired from Sobhan Pharmaceutical Company located in Tehran, Iran. Analytical-grade chemical reagents were procured from either Merck or Sigma-Aldrich. A solution of CLZP with a concentration of 1×10^{-3} M was created by dissolving the necessary amount of CLZP in methanol, then diluting it with double-distilled water and storing it at a temperature of 5 °C. Britton-Robinson buffer solutions with varying pH levels were prepared using H_3BO_3, acetic acid, and H_3PO_4. A pharmaceutical CLZP tablet containing 2 mg was obtained from a local pharmacy, and all solutions were made using double-distilled water. Electrochemical measurements were conducted using a Palmsense device with a conventional three-electrode system consisting of a saturated Ag/AgCl reference electrode, a screen-printed carbon electrode as the working electrode (either unmodified or modified with MXE), and a platinum plate counter electrode. pH measurements were performed using a Metrohm model 827 pH/mV meter. Electrochemical tests were carried out using a Palmsense apparatus equipped with a standard three-electrode setup, which included a saturated Ag/AgCl reference electrode, a screen-printed carbon

electrode as the working electrode (either unaltered or enhanced with MXE), and a platinum plate counter electrode. The pH readings were taken using a Metrohm model 827 pH/mV meter.

2.2 Preparation and synthesis

2.2.1 MXE preparation

The synthesis of MXE was conducted according to the procedures outlined in reference [31]. Briefly, 0.5 g of Ti_3AlC_2 MAX powder was slowly added to 10 mL of 30% hydrofluoric acid (HF) (ACROS Organics, $48-51\%$ solution in water) while stirring gently for 7 hours. The resulting solution underwent a single wash with deionized (DI) water through centrifugation at 3500 rpm for 30 minutes, followed by decanting the water-like supernatant. Subsequently, the residue underwent multiple washes with over 5 liters of DI water using vacuum-assisted filtration with a polyvinyl difluoride (PVDF) filter membrane (Durapore, Millipore) with a pore size of 0.22 μm until reaching a pH of 6.5, followed by drying under vacuum for 24 hours. In the delamination procedure, a mixture of 100 mg of $Ti_3C_2T_x$ powder and 20 mL of Diary of solution was stirred for 24 hours. Page 5 of 30 Diary of Materials Chemistry C6 tetramethylammonium hydroxide (TMAOH) (Alfa Aesar, Electronic Review, 99.9999% (metal premise) fluid) After stirring, the mixture was centrifuged at 5000 rpm for 30 minutes to isolate the undesired brown solution with TMAOH. This centrifugation process was repeated several times until the pH of the liquid above reached 7. Subsequently, the MXE solution underwent centrifugation at 3500 rpm for 5 minutes to isolate larger unetched particles, yielding a stable MXE colloidal solution suitable for further use [32].

2.2.2 Preparation of the modified electrode

The modified electrodes were prepared using a simple casting method. To create the MXE suspension, 2 mg of MXE was added to 2.0 mL of Dimethylformamide. The mixture was then sonicated at room temperature for 20 minutes to ensure a well-dispersed solution. Subsequently, 4 μL of this mixture were directly applied onto the surface of the screen-printed carbon electrodes and left to dry at room temperature.

2.3 Sample preparation

The human blood samples utilized in this research were sourced from Mehrad Hospital in Tehran, Iran, and kept frozen until required. To provide the serum sample, 2 mL of methanol was introduced to 5 mL of the serum as a protein precipitation agent. The mixture was vortexed for 5 minutes and then centrifuged at 4000 rpm for 15 minutes to separate the precipitated proteins. The clear supernatant layer was filtered through a 0.45 mm filter to obtain protein-free human serum, which was stored and used in the research process. Ten tablets, each containing 2 mg of CLZP, were acquired from Tehran Darou to prepare CLZP tablets. The tablets were meticulously weighed and finely ground into a powder. A specific amount of the powdered substance, equal to a 1×10^{-3} M CLZP stock solution, was added to a 50 mL beaker and dissolved in 10 mL of methanol by shaking for 10 minutes. The resulting solution was then filtered into a 25 mL calibrated flask. The residual powder in the beaker was washed thrice with methanol and combined with the flask contents. Subsequently, the volume was adjusted with BR (pH 3) to achieve the desired concentration, and the solution was preserved at 5 °C for future utilization.

3. Results and discussion

3.1 $TiAlC_2$ and TiC_2T_x properties

The shape and structure of the produced MXE were examined using XRD and SEM methods (figures 1 and 2). A distinct, well-stacked layered structure was visible on the Ti_3AlC_2 surface (figure 1 A). The etching reaction led to the formation of an accordion-like multilayer structure of MXE after the removal of Al from Ti_3AlC_2 (figure 1 B) [28, 29]. XRD patterns were utilized to examine the composition of the $Ti_3C_2T_x$ and Ti_3AlC_2 phases, both before and after HF treatment (figure 2). The crystalline Ti_3AlC_2 planes (0 0 2), (0 0 4), (1 0 1), (1 0 4), and (1 0 5) correlated with the diffraction peaks of MXE at 9.72, 19.32, 34.28, 39.24, and 41.92, respectively. The disappearance of engraved Al was confirmed at the 2θ position of approximately 39.24°, specifically on the (1 0 5) planes of crystalline Ti_3AlC_2, indicating the presence of exfoliated $Ti_3C_2T_x$ layers. Moreover, the shifting of the (0 0 2) peak to a smaller angle ($2\theta \approx 7.72°$) and its increased size compared to the XRD pattern of Ti_3AlC_2 provided evidence of the successful separation of $Ti_3C_2T_x$ layers [30, 31]. The presence of additional peaks corresponding to the (0 0 4), (0 0 6), (0 0 8), (0010), (0012), and (1 1 0) planes further supports the exfoliation of $Ti_3C_2T_x$ using the LiF protocol [32]. Additionally, energy dispersive X-ray spectroscopy (EDS) mapping confirmed the presence of oxygen, titanium, and carbon elements on the MXE/GCE surface, validating that C and Ti are primarily linked to MXE on the embedded surface (figure 1 C).

3.2 Electrochemical characterization of the different electrodes

To study the electrochemical reduction of clonazepam and evaluate the electrocatalytic activity, cyclic voltammograms (CVs) were obtained at modified and unmodified electrodes. These CV measurements were conducted in a BR solution with a pH of 3, containing 100 μM of clonazepam. The scan rate used was 100 mV/s, and the applied potential range varied from -0.1 to -0.9 V (see figure 3). The results show that the unmodified electrodes exhibit a very weak reduction peak potential at 0.48 V and a cathodic current density of about 2 μA, indicating an inability to reduce clonazepam. In contrast, the modified electrode with MXE exhibited a major high-intensity peak at 0.37 V with a current amplitude of 29 μA, attributed to the electrocatalytic reduction of CLZP due to the higher electrochemically active surface area of the modified electrode.

3.3 pH investigation

An investigation was conducted to examine the impact of solution pH on the oxidation of 50 μM CLZP at the modified screen-printed carbon electrodes. The study utilized a BR

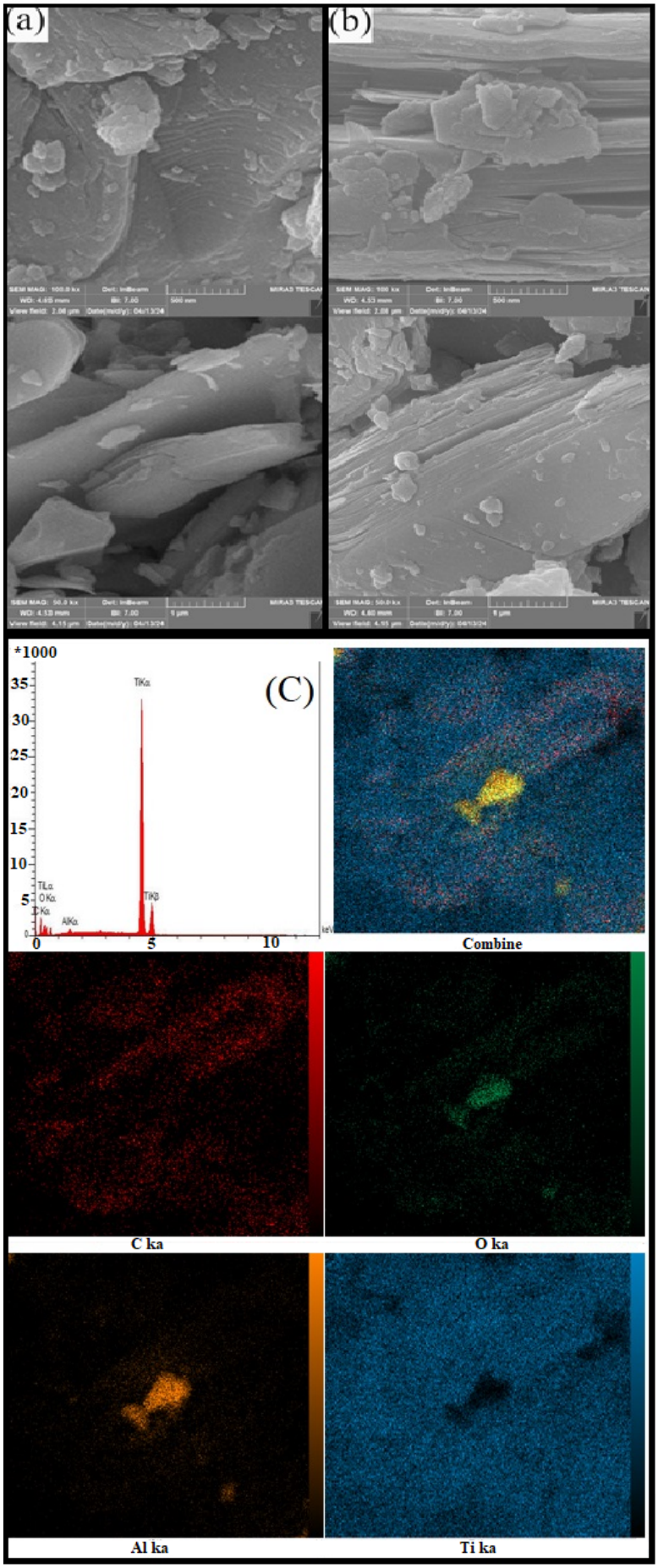

Figure 1. FESEM images of MXE before HF treatment (A), after HF treatment (B), (C) EDS and mapping.

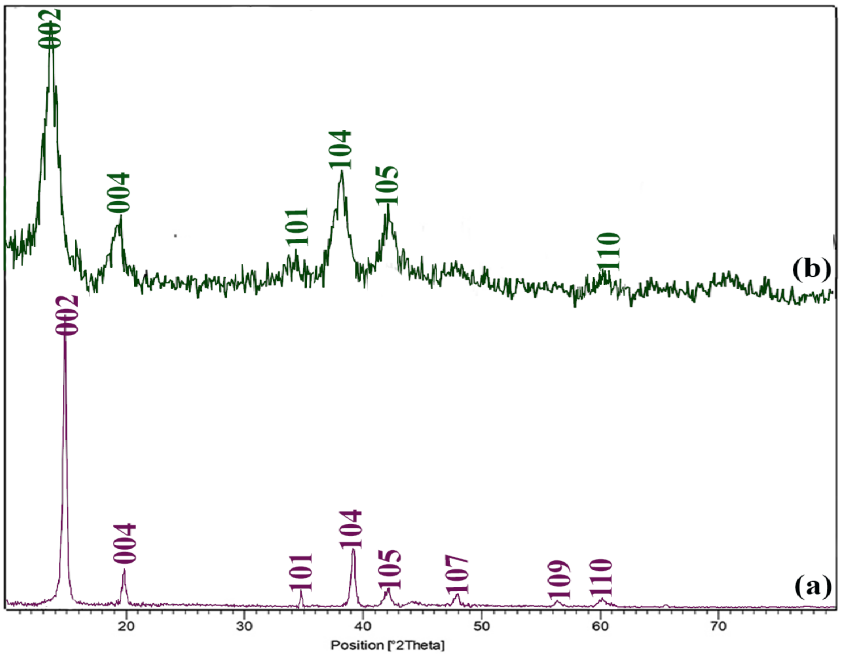

Figure 2. XRD patterns of $Ti_3C_2T_x$ and Ti_3AlC_2.

buffer solution with pH levels ranging from 3 to 7. The results, presented in figure 4, indicate that the electrode signal decreased as the pH increased from 3 to 7. Consequently, the highest signal was observed at pH 3. Therefore, a pH of 3 was chosen for all subsequent tests. Additionally, it was observed that increasing the pH caused the oxidation peak potential of CLZP to shift towards negative values, suggesting the involvement of H^+ in the oxidation process. When Ep is plotted against pH, a linear section with a gradient of 0.054 mV pH^{-1} was observed, indicating proximity to the Nernstian value of 0.59 mV pH^{-1} [32–38]. This finding suggests that the quantity of electrons involved in CLZP reduction is equivalent to the number of protons. According to these voltammograms, the nitro group of CLZP was first reduced to the related hydroxylamine group, and the probable mechanism is shown in scheme 1.

3.4 Effect of scan rate

To study the kinetics of the modified electrode, we examined the impact of potential scan rates (v) on the reduction peak current response to 100 μM CLZP using the CV method. The experiments were conducted in a BR solution (pH = 3) with scan rates varying from 10 to 150 mV/s. As the scan rate rose, the anodic peak currents of CLZP also increased. A linear correlation was observed between the square root of the scan rate ($\upsilon^{1/2}$) and the reduction peak current of CLZP,

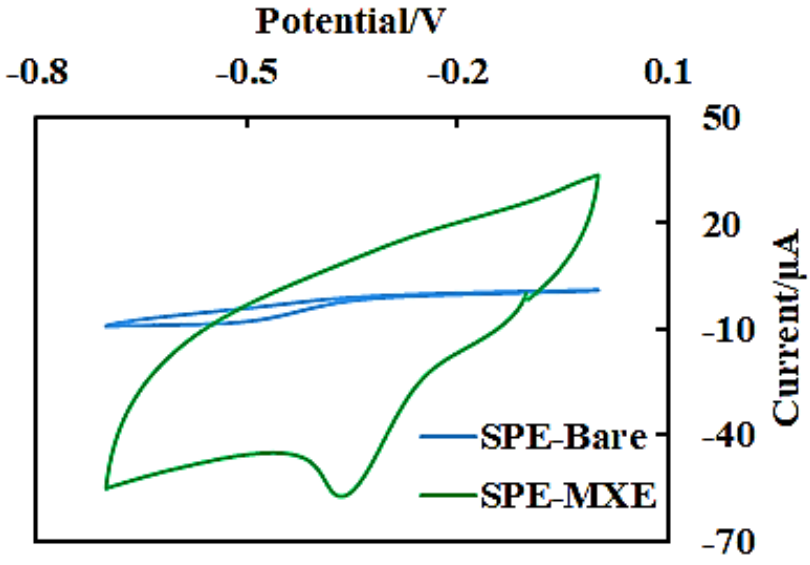

Figure 3. CVs of modified and unmodified screen-printed carbon electrodes in 100 μM CLZP at a scan rate of 100 mV/s.

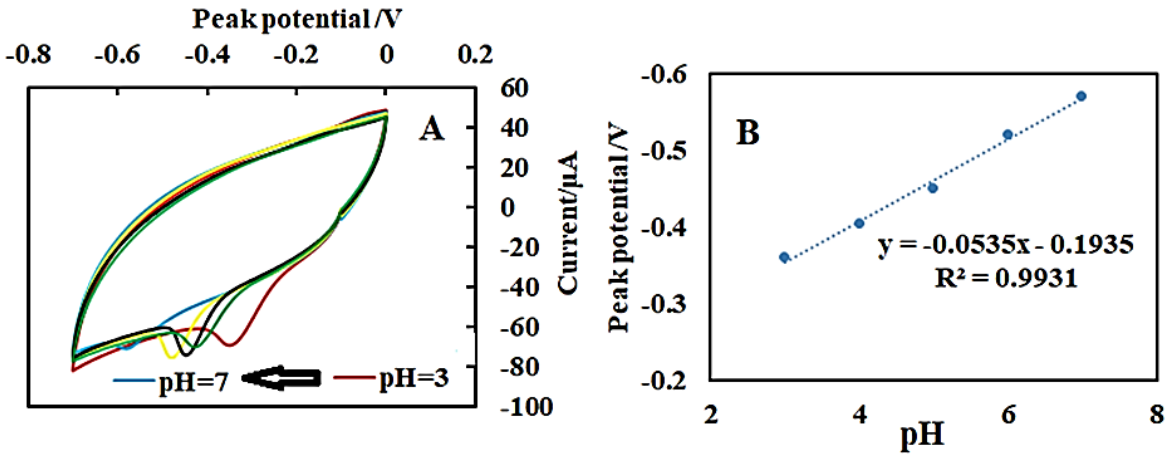

Figure 4. (A) CVs obtained in SPE/MXE electrode at different pH values containing 100 μM CLZP with a scanning speed of 100 mV/s. (B) Graphs of the anodic peak potential (Epa) versus different pH values.

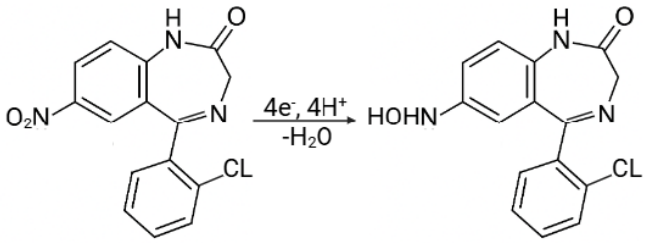

Scheme 1. Proposed mechanism for electrochemical reduction of CLZP.

suggesting that the oxidation of CLZP on the modified electrode is controlled by diffusion (figure 5).

3.5 Differential pulse voltammetry detection of CLZP at SPE/MXE electrode

The SPE/MXE electrode was able to detect CLZP under optimal conditions in BR (pH = 3) within the potential range of −0.1 to −0.8 V using DPV. DPV was chosen due to its lower contribution of charging current to the background current, higher sensitivity, and greater applicability compared to CV for estimating lower detection limits. Figure 6 displays the differential pulse voltammograms obtained with various CLZP concentrations using the SPE/MXE electrode. The calibration plot shown in

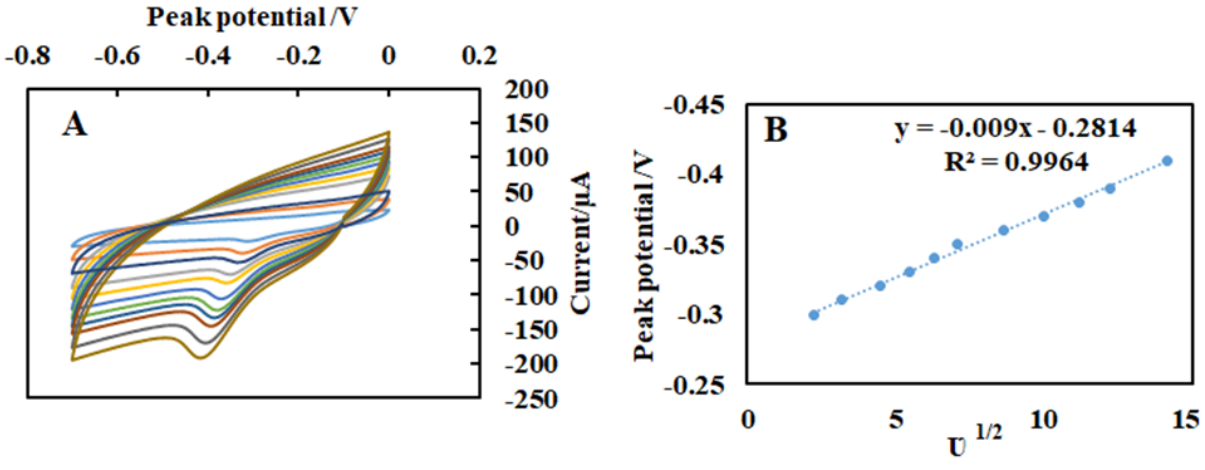

Figure 5. (A) CVs of 100.0 μM CLZP at the SPE/MXE electrode with different scan rates (10 to 150) at pH 3.0. (B) plot of peak current versus the square of the scan rate.

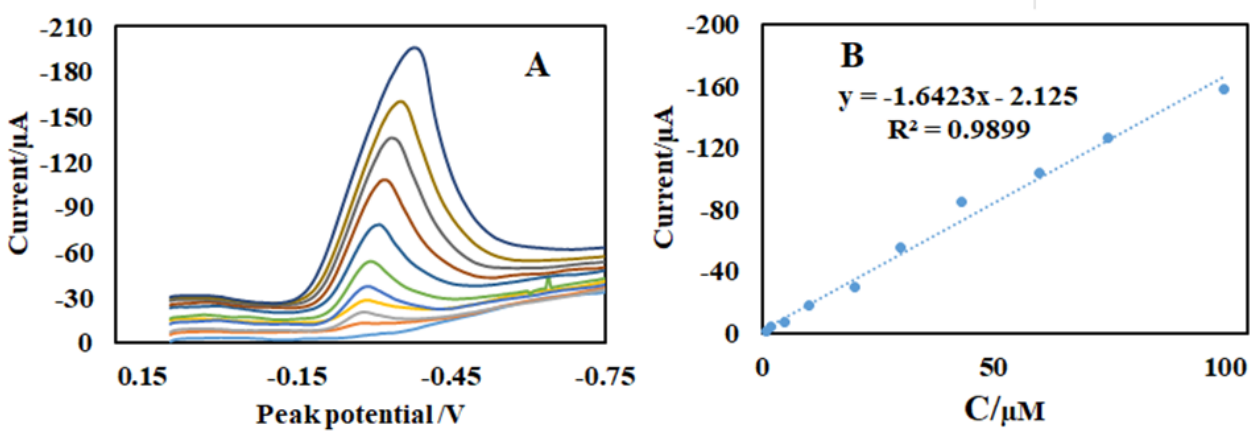

Figure 6. (A) Differential pulse voltammograms at the SPE/MXE electrode at pH 3.0 containing different concentrations of the target drug (1 to 100.0 μM). (B) Plot of peak reduction currents as a function of CLZP concentration.

figure 6 B exhibited good linearity within the CLZP concentration range of 1 to 100 μM. The limit of detection [39] was calculated as 3 Sb/m, where Sb represents the blank standard deviation and m is the slope of the calibration graph. The results show that the detection limit of the manufactured electrode is 0.3 μM and its linear range is $1-100$ μM.

3.6 Determination of CLZP in pharmaceutical formulations and human blood serum samples

To assess the effectiveness of the suggested electrochemical sensor, the analysis of CLZP in pharmaceutical formulations and human urine was conducted using the standard addition technique. Table 1 displays the retrieval of CLZP in these samples. The findings from the retrieval experiments illustrate the effective use of the adapted electrode for quantifying CLZP in pharmaceutical formulations and human serum samples. The findings indicate that the proposed method is simple, fast, and cost-effective, with a relatively good detection limit and a wide linear range. This effective performance can be attributed to the optimal fixation of MXE on the surface of the carbon electrode, which provides a large surface area, excellent conductivity, and useful electrocatalytic effects. Based on the available literature, Table 2 is a comprehensive comparison of electrochemical sensing methods for Clonazepam detection [40].

3.7 Interference study

The influence of various substances such as NaCl, KCl, glucose, dopamine, uric acid, and ascorbic acid that could potentially interfere with the determination of CLZP was evaluated under optimal experimental conditions. Different substances commonly found in pharmaceutical formulations and real samples were added to a solution containing 100.0 μM RZB in 0.1 M BR solution at pH 3. It was observed that the presence of different interferences did not affect the current response of CLZP. The findings demonstrated that the suggested approach exhibits exceptional selectivity when it comes to detecting CLZP in real samples.

3.8 Stability, repeatability, and reproducibility of the modified electrode

The stability, repeatability, and reproducibility of the SPE/MXE were assessed through DPV measurements of a 50.0 μM concentration of CLZP. The relative standard deviation (RSD%) was observed to be 4.6% over five successive assays. Furthermore, when four different electrodes were used for four measurement assays, the RSD% was determined to be 4.8%. In order to evaluate the stability of the electrode, it was stored at room temperature in the laboratory for a period of three weeks. Subsequent DPV measurements were compared with those obtained prior to storage. The findings indicated only a minor change in the peak current, suggesting that the modified electrode exhibited favorable stability, reproducibility, and repeatability.

Table 1. Determination results of CLZP in tablet and human serum samples.

Sample	Labeled (mg)	Result (mg)	Recovery%	RSD%
CLZP	1.0	0.90	90.20	3.0
	2.0	1.85	92.50	3.6
	4.0	3.50	87.65	4.1
Serum	5	4.8	96.4	2.1
	7	71.6	102.3	1.8

Table 2. Comparison of the sensing performance of different fabricated CLZP sensors.

Electrode type	Linear range	Detection limit	Technique	Sample type	Reference
Mercury drop electrode	1×10^{-7} to 1×10^{-5} M	1.3×10^{-8} M	SWCSV	Tablets	[41]
Glassy carbon electrode	6.3 – 31.5 pg/mL	3.3 μg/mL	Flow injection analysis	Tablet and urine	[42]
Changing Mercury drop electrode	Up to 550 ng/mL	10 ng/mL	DPAdSV	Urine (after extraction)	[43]
Modified carbon-paste electrodes	0.025 – 3.0 μg/mL	0.021 μg/mL	DPV	Plasma and urine	[44]
SPE/MXE	1 – 100 μM	0.3 μM	DPV	Serum and tablets	Current study

4. Conclusion

We have developed an effective MXE-based detection platform for analyzing clonazepam in pharmaceutical formulations and biological samples. Electrochemical testing revealed significant catalytic activity of the MXE-coated screen-printed carbon electrodes toward clonazepam reduction, characterized by enhanced peak currents and reduced peak potential. The SPE/MXE electrode demonstrated exceptional performance metrics, including sensitivity (1.64 μA/μM), selectivity, reproducibility, and stability. Operating across a linear range of 1 to 100 μM with a detection limit of 0.3 μM, this sensor provides a practical tool for precise clonazepam identification in real samples.

Ethical approval
This study was approved by the NIMAD research ethics committee (ID: IR.NIMAD.REC.1400.038).

Authors contributions
Authors have contributed equally in preparing and writing the manuscript.

Availability of data and materials
The data that support the findings of this study are available from the corresponding author, upon reasonable request.

Conflict of interests
The author declare that they have no known competing financial interests or personal relationships that could have appeared to influence the work reported in this paper.

Funding
The study described in this paper was supported by the Elite Researcher Grant Committee under award number 4000400 (IR.NIMAD.REC.1400.038) from the National Institutes for Medical Research Development (NIMAD), Tehran, Iran.

References

[1] C.P. Walker and S. Deb. *J. Pharm. Pract.*, **34**(2021):648–652. DOI: https://doi.org/10.1177/0897190019882880.

[2] A. L. D'Orazio, A. L. Mohr, A. Chan-Hosokawa, C. Harper, M. A. Huestis, J. F. Limoges, A. K. Miles, C. E. Scarneo, S. Kerrigan, L. J. Liddicoat, and K. S. Scott. *J. Anal. Toxicol.*, **45**(2021):529–536. DOI: https://doi.org/10.1093/jat/bkab064.

[3] H. Basit and C. I. Kahwaji. *StatPearls*, (2020):Clonazepam.

[4] O. Nguele. *Pharm. Pract.*, **19**(2021):1–12. DOI: https://doi.org/10.7439/ijpr.

[5] K. Jeanne Dit Fouque, C. E. Ramirez, R. L. Lewis, J. P. Koelmel, T. J. Garrett, R. A. Yost, and F. Fernandez-Lima. *Anal. Chem.*, **91**(2019): 5021–5027. DOI: https://doi.org/10.1021/acs.analchem.8b04979.

[6] J. Zhu, Y. Niu, and Z. Xiao. *Food Chem.*, **339**(2021):128136. DOI: https://doi.org/10.1016/j.foodchem.2020.128136.

[7] G. Corso, O. DApolito, M. Gelzo, G. Paglia, and A. D. Russo. *Bioanalysis*, **2**(2010):1883–1891. DOI: https://doi.org/10.4155/bio.10.149.

[8] S. Nanaware, A. Nayak, and A. P. Jain. *J. Adv. Sci. Res.*, **12**(2021): 166–170. DOI: https://doi.org/10.20959/wjpr20181-10586.

[9] N. M. Fayek, M. A. Farag, A. R. Abdel Monem, M. Y. Moussa, S. M. Abd-Elwahab, and N. D. El-Tanbouly. *J. Chromatogr. Sci.*, **57**(2019): 349–360. DOI: https://doi.org/10.1093/chromsci/bmz006.

[10] M. Shyamsundar, S. K. Chauthe, L. Subramani, M. A. Subbaiah, A. Gupta, L. Bajpai, M. Bagadi, and A. Mathur. *Sep. Sci. Plus.*, **4**(2021):16–23. DOI: https://doi.org/10.1002/sscp.202000046.

[11] J. M. van den Ouweland and I. P. Kema. *J. Chromatogr. B*, **883**(2012): 18–32. DOI: https://doi.org/10.1016/j.jchromb.2011.11.044.

[12] S. Lotfi and H. Veisi. *Mater. Sci. Eng. C.*, **103**(2019):109754. DOI: https://doi.org/10.1016/j.msec.2019.109754.

[13] Z. Jahromi, M. Afzali, A. Mostafavi, R. Nekooie, and M. Mohamadi. *Iran. Polym. J.*, **29**(2020):241–251. DOI: https://doi.org/10.1007/s13726-020-00788-7.

[14] H. Ashrafi, M. Hasanzadeh, K. Ansarin, S. A. Ozkan, and A. Jouyban. *Int. J. Biol. Macromol.*, **120**(2018):2466–2481. DOI: https://doi.org/10.1016/j.ijbiomac.2018.09.017.

[15] H. Boulaiz, P. J. Alvarez, A. Ramirez, J. A. Marchal, J. Prados, F. Rodríguez-Serrano, M. Perán, C. Melguizo, and A. Aranega. *Int. J. Mol. Sci.*, **12**(2011):3303–3321. DOI: https://doi.org/10.3390/ijms12053303.

[16] X. Zhang, X. Cheng, and Q. Zhang. *J. Energy Chem.*, **25**(2016): 967–984. DOI: https://doi.org/10.1016/j.jechem.2016.11.003.

[17] F. D. Guerra, M. F. Attia D. C. Whitehead, and F. Alexis. *Molecules*, **23**(2018):1760. DOI: https://doi.org/10.3390/molecules23071760.

[18] S. S. Hussain, M. S. Kamal, and M. K. Hossain. *J. Nanomater.*, **2019**(2019):1–17. DOI: https://doi.org/10.1155/2019/1562130.

[19] V. Torres-Costa. *Nanomaterials*, **12**(2022):1820. DOI: https://doi.org/10.3390/nano12111820.

[20] A. Khoshroo, L. Hosseinzadeh, A. Sobhani-Nasab, M. Rahimi-Nasrabadi, and F. Ahmadi. *Microchem. J.*, **145**(2019):1185–1190. DOI: https://doi.org/10.1016/j.microc.2018.12.049.

[21] Z. Wang and Z. Dai. *Nanoscale*, **7**(2015):6420–6431. DOI: https://doi.org/10.1039/C5NR00585J.

[22] X. Luo, A. Morrin, A. J. Killard, and M. R. Smyth. *Electroanalysis*, **18**(2006):319–326. DOI: https://doi.org/10.1002/elan.200503415.

[23] A. A. Ansari, M. Alhoshan, M. S. Alsalhi, and A. S. Aldwayyan. *Biosens. Bioelectron.*, **26**(2010):23–46. DOI: https://doi.org/10.5772/7201.

[24] J. Zhao, G. Chen, L. Zhu, and G. Li. *Electrochem. Commun.*, **13**(2011):31–33. DOI: https://doi.org/10.1016/j.elecom.2010.11.005.

[25] V. S. Manikandan, B. Adhikari, and A. Chen. *Analyst*, **143**(2018): 4537–4554. DOI: https://doi.org/10.1039/C8AN00497H.

[26] M. Khan, O. Ozalp, M. Khan, and M. Soylak. *J. Mol. Liq.*, **368**(2022): 120685. DOI: https://doi.org/10.1016/j.molliq.2022.120685.

[27] G. Kholafazadehastamal, M. Khan, M. Soylak, and N. Erk. *Carbon Lett.*, **34**(2024):929–940. DOI: https://doi.org/10.1007/s42823-023-00611-2.

[28] M. Khan and M. Soylak. *Microchem. J.*, **185**(2023):108200. DOI: https://doi.org/10.1016/j.microc.2022.108200.

[29] Q. Wang, N. Han, Z. Shen, X. Li, Z. Chen, Y. Cao, W. Si, F. Wang, B. J. Ni, and V. K. Thakur. *Nano Mater. Sci.*, **5**(2023):39–52. DOI: https://doi.org/10.1016/j.nanoms.2022.07.003.

[30] X. Wu, P. Ma, Y. Sun, F. Du, D. Song, and G. Xu. *Electroanalysis*, **33**(2021):1827–1851. DOI: https://doi.org/10.1002/elan.202100192.

[31] T. B. Limbu, B. Chitara, J. D. Orlando, M. Y. Cervantes, S. Kumari, Q. Li, Y. Tang, and F. Yan. *J. Mater. Chem. C.*, **8**(2020):4722–4731. DOI: https://doi.org/10.1039/C9TC06984D.

[32] Z. Khorablou, F. Shahdost-Fard, and H. Razmi. *Microchem. J.*, **193**(2023):109216. DOI: https://doi.org/10.1016/j.microc.2023.109216.

[33] T. Anusha, K. S. Bhavani, J. S. Kumar, A. Bonanni, and P. K. Brahman. *Microchem. J.*, **161**(2021):105789. DOI: https://doi.org/10.1016/j.microc.2020.105789.

[34] P. K. Brahman, R. A. Dar, and K. S. Pitre. *Arab. J. Chem.*, **9**(2016): S1884–S1888. DOI: https://doi.org/10.1016/j.arabjc.2012.08.007.

[35] P. K. Kalambate, Dhanjai, A. Sinha, Y. Li, Y. Shen, and Y. Huang. *Microchim. Acta.*, **18**(2020):1–12. DOI: https://doi.org/10.1007/s00604-020-04366-9.

[36] A. L. Lavanya, K. G. Bala Kumari, K. R. Prasad, and P. K. Brahman. *Int. J. Environ. Anal. Chem.*, **102**(2022):720–735, . DOI: https://doi.org/10.1080/03067319.2020.1726333.

[37] A. L. Lavanya, K. G. Kumari, K. R. Prasad, and P. K. Brahman. *Electroanalysis*, **33**(2021):1096–1106, . DOI: https://doi.org/10.1002/elan.202060524.

[38] W. Niamsi, N. Larpant, P. K. Kalambate, V. Primpray, C. Karuwan, N. Rodthongkum, and W. Laiwattanapaisal. *Biosensors*, **12**(2022): 852. DOI: https://doi.org/10.3390/bios12100852.

[39] K. Thongprasom, M. Carrozzo, S. Furness, and G. Lodi. *Cochrane Database Syst. Rev., 2011 (7). DOI: https://doi.org/*, **2011**(2011)(7). DOI: https://doi.org/10.1002/14651858.CD001168.pub2.

[40] K. C. Honeychurch. *Biosensors*, **9**(2019):130. DOI: https://doi.org/10.3390/bios9040130.

[41] C. M. dos Santos, V. Famila, and S. M. Gonçalves. *Anal. Bioanal. Chem.*, **374**(2002):1074–1081. DOI: https://doi.org/10.1007/s00216-002-1535-0.

[42] C. Latorre, M. H. Blanco, E. L. Abad, J. Vicente, and L. Hernández. *Analyst*, **113**(1988):317–319. DOI: https://doi.org/10.1039/AN9881300317.

[43] A. Zapardiel, J. A. Pérez López, E. Bermejo, L. Hernandez, and A. G. Espartero. *Anal. Lett.*, **24**(1991):233–248. DOI: https://doi.org/10.1080/00032719108052900.

[44] M. E. Lozano-Chaves, J. M. Palacios-Santander, L. M. Cubillana-Aguilera, I. Naranjo-Rodríguez, and J. L. Hidalgo-Hidalgo de Cisneros. *Sens. Actuators B Chem.*, **115**(2006):575–583. DOI: https://doi.org/10.1016/j.snb.2005.10.021.